NASA TECHNICAL NOTE

NASA TN D-2064

A STUDY OF THE CONVECTIVE AND RADIATIVE HEATING OF SHAPES ENTERING THE ATMOSPHERES OF VENUS AND MARS AT SUPERORBITAL SPEEDS

by Fred A. Demele

Ames Research Center
Moffett Field, California

NATIONAL AERONAUTICS AND SPACE ADMINISTRATION • WASHINGTON, D. C. • DECEMBER 1963

A STUDY OF THE CONVECTIVE AND RADIATIVE HEATING OF SHAPES ENTERING THE ATMOSPHERES OF VENUS AND MARS AT SUPERORBITAL SPEEDS

By Fred A. Demele

Ames Research Center
Moffett Field, Calif.

NATIONAL AERONAUTICS AND SPACE ADMINISTRATION

A STUDY OF THE CONVECTIVE AND RADIATIVE HEATING OF . . . . ENTERING THE ATMOSPHERES OF VENUS AND MARS AT SUPERORBITAL SPEEDS

By Fred A. Demele

SUMMARY

An analytical study is made of the radiative and convective heating encountered by a short 10° half-angle blunt capsule and by sharp conical shapes entering assumed atmospheres of Venus and Mars at superorbital speeds. A simplified theoretical analysis is adopted for the convective mode, whereas experimental shock-layer radiation is utilized for the radiative mode.

The analysis indicates that for blunt capsule entries at speeds somewhat greater than the Hohmann transfer planetary arrival velocities, the predominant heating mode is by radiation in the case of Venus and by convection in the case of Mars. It is shown that sweepback of the bow shock can reduce the radiative input so drastically that for Venus entry the total combined radiative and convective heat input of a conical shape will be about half that of a blunt capsule. Because convective heating predominates in the Mars entry, little or no reduction in total heat is afforded by conical shapes. However, since the radiation is highly dependent on velocity, conical shapes appear attractive for Mars entry at higher velocities (say 40,000 ft/sec) corresponding to those for shortened interplanetary trip times. There is strong experimental evidence that the intensity of radiation is significantly influenced by gas composition. It follows, therefore, that for blunt capsule entries wherein the radiative heating predominates, the total heat input similarly is strongly dependent on the gas composition. In contrast, the total heat input to optimum conical shapes does not vary significantly with gas composition in the Venus and Mars atmospheres.

INTRODUCTION

One of the challenging problems confronting the designer of missiles and entry vehicles is that of aerodynamic heating. It has been long recognized (e.g., ref. 1) that when the predominant mode of heating is convection, as in satellite entries, the heat input can be minimized if a large ratio of pressure-to-friction drag is maintained, as afforded by blunt shapes. However, as entry speeds increase to parabolic values and above, the vehicle shock-layer temperature increases during entry, until the air in this region undergoes dissociation and finally ionization. The shock-layer gas then emits energy by radiation, which can be a significant component of the total heat input. For spherical nose shapes the radiation has been found to decrease rather rapidly away from the stagnation region and, further, to be proportional to the shock standoff distance, so that a small nose radius is desirable to minimize the radiative heat input to the vehicle. Reference 2 has demonstrated the desirability of using sharp

conical shapes to suppress the radiative heat input at velocities much greater than parabolic. The concept is analogous to using sweepback for reducing compressibility effects; namely, the radiation intensity is dependent on the velocity normal to the bow shock, rather than on the free-stream velocity. Optimum cone angles are developed in reference 2 for Earth entry velocities ranging from about 10 to 30 km/sec, for an ablating heat shield. The shapes were assumed to remain conical during ablation.

For entry into planetary atmospheres other than Earth's (e.g., Mars and Venus), the results of reference 2 are not directly applicable, since the thermochemical structures of these atmospheres appear to differ significantly from that of Earth (see, e.g., ref. 3). Not only are there differences in atmospheric pressures, temperatures, and scale heights, but the constituents of the atmospheres of Venus and Mars seem to be mainly nitrogen and carbon dioxide as opposed to air. Experimental studies being conducted at Ames Research Center (see ref. 4) give evidence of much higher radiation intensities from N_2 - CO_2 mixtures representative of those conjectured for Venus and Mars than from air. Futhermore, the speeds of entry of early planetary probes into those atmospheres will likely be at least a little greater than those associated with minimum energy interplanetary transits (i.e., about 35,000 ft/sec for Venus and about 20,000 ft/sec for Mars). However, as booster capabilities increase, it may be desirable to diminish the transit times, thereby increasing the planetary arrival velocities. Under these circumstances, radiation can be the dominant mode of heating and must be reckoned with by the designer. The significance of such increased radiation relative to the total heating encountered by shapes entering assumed atmospheres of Venus and Mars is the subject of concern in the present report.

The shapes studied were a short 10° half-angle blunted conical body and sharp conical bodies with half-angles varying from 15° to 55°. Radiative and convective heat inputs are presented for steep entries at 37,500 and 50,000 ft/sec for Venus and 26,000 and 40,000 ft/sec for Mars, generally for assumed atmospheres composed of 7-1/2 percent CO_2 and the remainder N_2. However, the effect of gas composition on total heat inputs to both shapes is also examined.

NOTATION

A reference area, $\frac{\pi D^2}{4}$

C constant in stagnation-point laminar convective heating equation

C_D drag coefficient, $\frac{\text{drag}}{(1/2)\rho_\infty V_\infty{}^2 A}$

$C_D{}^*$ reference drag coefficient (value for blunt capsule and for 36° half-angle cone)

D base diameter

E_t total radiation flux per unit volume of gas in the shock layer

h altitude

k	constant relating radiant intensity to density and velocity
m	vehicle mass
p	ambient pressure
$\dot{q}_c$	laminar convective heat-transfer rate
$\dot{q}_{c_o}$	stagnation-point laminar convective heat-transfer rate
$\dot{q}_{s_o}$	sonic-point turbulent convective heat-transfer rate
$\dot{q}_r$	radiative heat-transfer rate
$\dot{q}_{r_o}$	stagnation-point radiative heat-transfer rate
$\dot{Q}_c$	total laminar convective heat-transfer rate
Q_c	total laminar convective heat input
$\dot{Q}_r$	total radiative heat-transfer rate
Q_r	total radiative heat input
Q_T	sum of convective and radiative heat input
R	nose radius
R_∞	free-stream Reynolds number
s	distance from apex along conical surface element
S	surface area
t	time measured from initiation of entry
T	temperature
V_E	entry velocity
V_∞	flight velocity
δ	shock-wave standoff distance
ρ_∞	free-stream density
ρ_2	density behind shock wave
$\rho_{o_\oplus}$	Earth sea-level density
θ_c	cone semivertex angle

θ_{opt} cone semivertex angle for minimum total heat input

θ_w shock-wave angle

γ_E flight-path entry angle

METHOD OF ANALYSIS

Trajectories

The entry trajectories for which the heating analysis has been made required the solution of planar motion equations for a point-mass body. The solutions were obtained numerically on an IBM 7090 computer. Inherent to this program was the assumption that the planets were spherical and nonrotating. The model atmospheres used (see fig. 1) are assumed profiles which have been included in various studies conducted by or for the Jet Propulsion Laboratory, and are based on information given in references 5 and 6. The following assumptions and conditions have been stipulated for the study:

	Venus	Mars
Planet radius	2.0341728×10^7 ft	1.1155109×10^7 ft
Surface gravity	28.21488 ft/sec^2	12.79512 ft/sec^2
Entry altitude	700,000 ft	1,000,000 ft
Entry velocity and transit time	37,500 ft/sec/105 days 50,000 ft/sec/58 days	26,000 ft/sec/135 days 40,000 ft/sec/97 days
Entry angle	-89°	-89°

Shapes Considered

Two types of shapes were studied herein, (1) a short 10° half-angle blunted conical body, and (2) sharp conical shapes with the same diameter as the blunted conical body. Dimensional sketches of both types are shown in figure 2. The aerodynamic characteristics of the blunted conical shape have been studied rather extensively experimentally (see refs. 7, 8, and 9) and the dynamic behavior of this shape during Martian entry was the subject of analysis in reference 10. Although the afterbodies of these shapes have important effects on aerodynamic stability and volume required, they contribute little to the total heat input; therefore, the present study ignores the afterbodies insofar as heating is concerned. For comparative purposes, both shapes are considered to have the same mass, namely 5.724 slugs. To determine the ballistic parameter, m/C_DA, the drag coefficient was calculated by Newtonian theory.

Convective Heating

It was recognized that a rigorous analysis of convective heating should account for thermodynamic and transport properties of the gas mixtures in the boundary layer, including the effects of gaseous dissociation and ionization. However, it appeared desirable to determine an approximate equation which could be expected to yield sufficiently accurate results for comparative heat analysis of shapes. The well-known stagnation heating-rate equation for air at conditions wherein the stagnation enthalpy is much greater than the wall enthalpy, $\dot{q}_{c_o}\sqrt{R} = C\rho_\infty^{1/2}V_\infty^3$ (see ref. 11), was found to satisfy this requirement for a value of $C = 20.4\times10^{-9}$ when $\dot{q}_{c_o}$ is given in Btu/ft^{2}sec. The results obtained with this equation agree well with experimental measurements in air and CO_2 (see ref. 12) at velocities up to 18,000 ft/sec, as shown in figure 3. In the velocity range from 20,000 to 50,000 ft/sec, the foregoing approximate equation was compared with the theory of Hoshizaki (ref. 13) and was found to differ by less than 10 percent. Since Hoshizaki's theory takes into account dissociation and ionization and yields satisfactory agreement with experimental heat-transfer data obtained in partially ionized air and CO_2, the approximate equation was adopted for use herein.

To evaluate the total heat input for a given shape, it is, of course, necessary to determine the local distribution of heating for the duration of entry, as seen by the following equation for total heat input:

$$Q_c = \int_t \int_S \dot{q}_{c_o}(\dot{q}_c/\dot{q}_{c_o})dt\ dS$$

The method of Lees (ref. 14) has been used to determine the local distribution of heating. As in the case of the stagnation heating-rate equation, the enthalpy at the wall is assumed to be much less than that at the boundary-layer edge, and the flow, laminar. The assumption of laminar flow seems reasonable for Mars entry, but is subject to uncertainty for Venus entry. In this connection, it can be seen in figure 4 that free-stream Reynolds numbers approaching 10^7 per foot occur during the Venus entries. However, these values occur well beyond the maximum heating pulse, and at the time of maximum heating, Reynolds numbers of 2 or 3×10^6 per foot are attained.

Radiative Heating

To assess the radiation of a gas at elevated temperatures, the spectral radiance of the chemical species must be known. The radiance of air in equilibrium has been quite well defined, both theoretically (ref. 15) and experimentally (ref. 16). However, the theoretical equilibrium radiation of CO_2 - N_2 mixtures presently believed to be representative of the atmospheres of Venus and Mars is not yet well defined. Therefore, the experimental shock-layer radiation data recently obtained in the Ames pilot hypersonic free-flight facility (see ref. 4)

have been used to assess the radiative heat input for a blunt capsule and for sharp conical shapes entering the Venus and Mars atmospheres.

The stagnation radiative flux of the blunt shape can be expressed by $\dot{q}_{r_o} = (E_t/2)\delta$ (e.g., ref. 17), where E_t is the total equilibrium radiation flux per unit volume in the stagnation region and δ is the shock standoff distance which can be evaluated by the expression, $\delta/R = 0.78\ \rho_\infty/\rho_2$ (see ref. 18). Wick has shown in reference 19 that a good average of the ratio of shock standoff distance to nose radius is 0.045 for air. It is recognized that differences in the density ratio at the shock wave exist between N_2 - CO_2 mixtures and air, particularly for conditions of high enthalpy. Analysis of this region for such mixtures is not considered herein, but should be the subject of further study. The total radiative input for the blunt shape can be expressed as

$$Q_r = \int_t \int_S \dot{q}_{r_o} (\dot{q}_r/\dot{q}_{r_o}) dt\ dS$$

which, in terms of the emitted radiation, can be expressed in the form

$$Q_r = \delta/2 \int_t \int_S E_t (\dot{q}_r/\dot{q}_{r_o}) dt\ dS$$

The quantity $\delta \int_S (\dot{q}_r/\dot{q}_{r_o}) dS$ represents an effective radiating volume of gas at stagnation-point conditions necessary to reproduce the total radiative heating. For the round nose models used in the experimental investigations of references 4 and 16 to obtain shock-layer radiation, the effective radiating volume for air was estimated (see ref. 16) on the basis of a constant shock-layer thickness and theoretical equilibrium radiation utilizing computed temperature and density distributions. The effective volume of the blunt capsule studied herein was obtained from the effective volume computed for the experimental models scaled by the cube of the ratio of capsule-to-model nose radius. Geometric differences do exist, in that the model nose terminated at approximately the sonic point, whereas the blunt capsule nose is more nearly a complete hemisphere. However, because the theoretical radiation flux at the sonic point was less than 10 percent of the stagnation value, neglecting the region behind the sonic point in calculating the effective shock volume of the capsule would appear to result in only a small error in the total radiative heat input. It should be noted that the experimental gas radiation, E_t, has been directly applied to the blunt capsule for identical conditions of free-stream density and velocity. For entry conditions outside the experimental range, the radiation has been assumed to vary in direct proportion to the free-stream density and exponentially with velocity to the eighth power, that is, $E_t = k\rho_\infty V_\infty^{\ 8}$. For the gas mixture assumed for most of the analysis (i.e., about 7-1/2-percent CO_2 and the remainder N_2), k has a value of 2.055×10^{-26} with E_t in the $Btu/ft^3 sec$, ρ_∞ in $slugs/ft^3$, and V_∞ in ft/sec. The assumed variation of equilibrium radiation with density and velocity is the present best estimate based on the experimental radiation data of reference 4, wherein the ambient pressure was varied from 3 to 60 mm Hg absolute and the model flight velocity was varied from 16,000 to 26,000 feet per second. It is recognized that at higher velocities, the radiation intensity may be dependent

on a velocity power other than 8 (as is the case with air), and therefore the results for the blunt capsule should be considered of a qualitative nature. Furthermore, at the lower densities there is evidence in the test results of nonequilibrium radiation. Since free-stream densities of about one hundredth those of the experimental data are encountered during the early portion of the radiative heat pulse, one might inquire of the validity of the density extrapolation. Following the arguments advanced in reference 20, it is assumed herein that the degree of completion of the chemical processes in the shock layer depends on the product of the density and a characteristic body length, say the radius. That is, nonequilibrium conditions during full-scale capsule entry and for small-scale tests should be concurrent when the product $\rho_\infty R$ and the velocity are the same for both. For the steep entries of the blunt capsule considered herein, the matching $\rho_\infty R$ for experimental conditions which are mainly in equilibrium occurs early in the radiative heating pulse. This is not the case for shallow entries wherein the densities are so low that nonequilibrium flow likely exists during a large part of the radiative heating pulse.

For the sharp cones, the temperature behind the shock is assumed to be constant over the length of the cone. Therefore, the equilibrium radiative flux to the surface can again be expressed by $\dot{q}_r = (E_t/2)\delta$, where the shock-layer thickness is seen from the adjacent sketch to be:

$$\delta = s \sin(\theta_w - \theta_c)$$

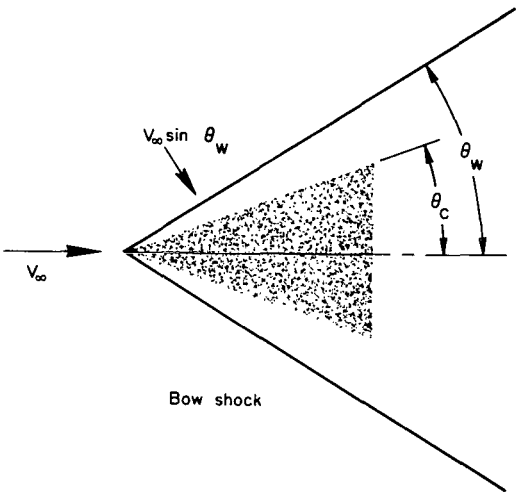

The total radiative heat input can then be expressed by the relation:

$$Q_r = \int_t \int_S (E_t/2)s \sin(\theta_w - \theta_c) dS\, dt$$

It will be recognized that the surface integral is simply the shock-layer volume, which is easily evaluated once the shock angle is determined. In the present analysis, the shock angles were determined for dissociated equilibrium air (ref. 21). Future study should include the definition of conical flows for CO_2 - N_2 mixtures. The sketch shows that the velocity contributing to the radiation is the free-stream component normal to the conical shock. It will be recalled that the experimental radiation intensity, E_t, is the blunt model stagnation value. Therefore, when the radiation data are applied to the sharp cones, the model velocity is matched with the free-stream component of velocity normal to the conical shock (i.e., $V_\infty \sin \theta_w$). Because of this velocity reduction, the experimental velocities for which radiation intensities were obtained were sufficiently high to encompass most of the entry conditions studied for the cones. As in the case of the blunt shape, the radiation has been assumed to vary in direct proportion to the free-stream density for entry conditions outside the experimental range. It is probable that, particularly during the entry conditions of low density previously noted, a region of nonequilibrium flow will prevail near the shock surface.

The problem of theoretically defining such an area is difficult both because of the complexity of the physics of the nonequilibrium processes, and because the relaxation along curved streamlines of the flow (see, e.g., ref. 22) must be computed. This problem as well as experimental radiation measurements of sharp cones should be studied to assess the validity of the assumptions made herein.

RESULTS AND DISCUSSION

Heating Rates

To illustrate the significance of radiative heating for Venus-Mars entry, time histories of stagnation-point convective and radiative heating rates for the blunt capsule are shown in figure 5. The accompanying trajectories are normal to the planet surface and have initial velocities of 37,500 feet per second for Venus and 26,000 feet per second for Mars, somewhat greater than the Hohmann transfer values in each case. It is evident that for the Venus entry shown, the radiative heating far exceeds the convective heating for the assumed capsule geometry during most of the period of significant heating. On the other hand, for the Mars entry shown, the convective heating dominates the radiative heating throughout the entry. The difference in the indicated relative importance of radiative heating is due, in part, to higher densities but mainly to the higher velocities associated with the Venus entry.

Time histories of total heat-transfer rate are shown in figure 6 both for the blunt capsule and for a cone having the same m/C_DA (i.e., $\theta_c = 36^o$). For the blunt capsule, the relative importance of radiative and convective heat input is similar to that indicated by the stagnation heating rates, although the ratio of radiative to convective heat input is less than the ratio of radiative to convective stagnation heating rate. For Venus entry, substantial reductions in combined radiative and convective heat input can be realized by the use of a sharp cone. On the other hand, for the Mars entry shown, the reduction in radiative heat input by use of a sharp cone is offset by the increase in convective heat input, indicating no advantage of the sharp cone over the blunt capsule from total heat considerations. It will be shown subsequently that significant reductions in total heat encountered during Mars entry can be realized by the use of a sharp cone, but at entry velocities much higher than the Hohmann transfer value.

Total Heat Input

Because the weight of heat protection of an entry vehicle is dependent on the total heat input, the following sections are concerned with considerations which influence the total heat. The manner in which the cone angle affects the convective, radiative, and combined total heat inputs is examined. Comparisons are then made between the total heat inputs to optimum cones and to the blunt capsule described earlier and, finally, the influence of gas composition is studied. In addition to the trajectories examined previously wherein the entry velocities were slightly higher than the Hohmann values, steep trajectories with entry

velocities representative of relatively short interplanetary trips, namely 50,000 ft/sec for Venus, and 40,000 ft/sec for Mars, were utilized in the studies.

Dependence on cone angle.- The effect of cone angle on convective, radiative, and combined total heat inputs is shown in figure 7 for Venus entry, and in figure 8 for Mars entry. The decrease in convective heating rate with increasing cone angle is largely due to the higher drag associated with increasing cone angle, since the convective heat varies inversely as the square root of the drag coefficient. The trends in drag coefficient (i.e., increase with increasing cone angle) and in shock-layer volume (reduction with increasing cone angle for a constant base diameter) tend to reduce the radiative heat input at the higher cone angles. However, the radiative heat increases with increasing cone angle as shown because of the large exponential dependence on the velocity component normal to the shock as noted earlier. An interesting finding is that at the optimum cone angle (i.e., the angle at which the combined heat input is a minimum), the radiative heat input is approximately 15 percent of the convective heat input. The result of increasing the ballistic parameter $m/C_D{}^*A$ of the vehicle is to increase the total heat as well as to lower the optimum cone angle. It will be recalled that the convective heating rate varies as $\rho_\infty{}^{0.5}$ and the radiative intensity as ρ_∞. For steep planetary entry the convective heat input likewise varies as $\rho_\infty{}^{0.5}$, or as $(m/C_DA)^{0.5}$, and the radiative heat input as ρ_∞, or as m/C_DA (see ref. 11 for development of the correspondence between ρ_∞ and m/C_DA). Thus, the greater dependence of radiative heat input on m/C_DA results in the lower optimum cone angles with increasing $m/C_D{}^*A$. It is further evident that entry at higher velocities results not only in increased total heat but in lower optimum cone angles, because radiative heating increases with velocity so much faster than convective heating. Thus, for Venus entry the optimum cone angle for a vehicle having $m/C_D{}^*A = 1$ would be about 35° for an entry velocity of 37,500 ft/sec (see fig. 7(a)) and about 27° for an entry velocity of 50,000 ft/sec (see fig. 7(b)). For Mars entry at 26,000 ft/sec (see fig. 8(a)), because the radiative heating is small, the optimum angle is large, being somewhat higher than 50° for an $m/C_D{}^*A = 1$. However, for the entry velocity of 40,000 ft/sec (see fig. 8(b)) the radiative heating is significant and the optimum cone angle is reduced to an average value of about 35° for the range of $m/C_D{}^*A$ shown. It may be noted by comparing Mars entry at 40,000 ft/sec (fig. 8(b)) with Venus entry at 37,500 ft/sec (fig. 7(a)) that although the optimum cone angles are about the same, significantly higher total heat is encountered during Mars entry. Since the atmosphere of Mars has a higher scale height than that of Venus (see fig. 1), the heating pulse during Mars entry is considerably longer than that for Venus entry. This effect, coupled with a higher initial velocity which tends to offset the effect of lower densities encountered in the Mars atmosphere, results in the higher total heat indicated.

Comparison of shapes.- The total heat input and the ratio of radiative to convective heat input of the blunt capsule and of optimum sharp cones are shown in figure 9 for Venus and Mars entry. The reductions in total heat input afforded by the use of sharp cones are seen to increase significantly with increasing $m/C_D{}^*A$. Since the majority of the heat input to the optimum sharp cones is by convection, the accompanying total heat increases roughly as $(m/C_D{}^*A)^{0.5}$. On the other hand, for blunt capsule entries wherein the radiative heating is large compared with the convective, the total heat increase approaches a first power variation with $m/C_D{}^*A$.

Effect of gas composition.- The results presented thus far pertain to a gas mixture having a volumetric composition of about 7-1/2 percent CO_2 and the remainder N_2. Since the intensity of radiation as shown in reference 4 depends on the relative abundance of CO_2 and N_2 in mixtures of these gases, it may be expected that the total heat input during entry and the optimum cone angle will depend on the gas composition. To examine this premise, calculations were made for gas mixtures ranging from pure N_2 to 70 percent N_2 - 30 percent CO_2, utilizing the experimental radiation data of reference 4, and the results are shown for Venus and Mars entry in figures 10 and 11, respectively. Although the absolute magnitudes are uncertain because of the preliminary nature of the experimental radiation data, the results give evidence of a maximum total heat input, and therefore a minimum optimum cone angle, occurring for a mixture containing between 10 and 15 percent CO_2. It is seen that the cone total heat is not strongly dependent on gas composition, primarily because the radiation heat input can be held small by optimizing the cone angle, that is, by utilizing smaller cone angles as the radiation intensity increases. On the other hand, the blunt capsule total heat varies considerably with gas composition, and for the gas composition of highest radiation, appears to be between two and three times as large as the cone total heat.

SUMMARY OF RESULTS

A study has been conducted of the convective and radiative heating associated with steep entry of a short 10° half-angle blunt capsule and sharp conical shapes into the atmospheres of Venus and Mars at velocities in excess of parabolic values. The principal results are:

1. For Venus entry at velocities somewhat above the Hohmann transfer value, the radiative heating to a blunt capsule appears significantly higher than the convective heating. However, on a conical shape the radiative input would be drastically less. For example, a cone of the same m/C_DA as the blunt capsule is indicated to have only about half the total heat input.

2. For Mars entry at velocities somewhat in excess of the Hohmann transfer value, convection is the predominant heating mechanism, and the shape of the capsule has little effect on the total heat. However, at much higher entry velocities, say 40,000 ft/sec, the heating of a blunt capsule is predominately by radiation, and, as in the case of Venus entry, large reductions in total heat input are indicated through the use of conical shapes.

3. The cone angle for minimum combined radiative and convective heat input decreases as the entry velocity is increased. The radiative input appears to be about 15 percent of the convective input when the cone angle is optimum.

4. The percentage of CO_2 in CO_2 - N_2 mixtures significantly influences the intensity of gaseous radiation, such that entries into planetary atmospheres having between 10 and 15 percent CO_2 and the remainder N_2 would be most severe from total heat considerations.

5. The total heat input to optimum conical shapes, in contrast to that of the blunt capsule, is not strongly dependent on gas composition, making such shapes further attractive for use in early planetary entries because of the uncertainty of gas constituents in the Venus and Mars atmospheres.

Ames Research Center
National Aeronautics and Space Administration
Moffett Field, Calif., Sept. 11, 1963

REFERENCES

1. Allen, H. Julian, and Eggers, A. J., Jr.: A Study of the Motion and Aerodynamic Heating of Ballistic Missiles Entering the Earth's Atmosphere at High Supersonic Speeds. NACA Rep. 1381, 1958.

2. Allen, H. Julian, Seiff, Alvin, and Winovich, Warren: Aerodynamic Heating of Conical Entry Vehicles at Speeds in Excess of Earth Parabolic Speed. NASA TR R-185, 1963.

3. Kellogg, William K., and Sagan, Carl: The Atmospheres of Mars and Venus. Publication 944, National Academy of Sciences, National Research Council, 1961.

4. James, Carlton S., and Smith, Willard G.: Experimental Studies of Static Stability and Radiative Heating Associated with Mars and Venus Entry. Proc. at IAS 31st Annual Meeting, New York, Jan. 1963, pp. 16-21.

5. Schilling, G. F.: Extreme Model Atmospheres of Mars. RM2782 - JPL, June 1961.

6. Kaplan, L. D.: A Preliminary Model of the Venus Atmosphere. Tech. Rep. 32-379, JPL, Dec. 1962.

7. Treon, Stuart L.: Static Aerodynamic Characteristics of Short Blunt Cones With Various Nose and Base Cone Angles at Mach Numbers From 0.6 to 5.5 and Angles of Attack to 180°. NASA TN D-1327, 1962.

8. Wehrend, William R., Jr.: Wind-Tunnel Investigation of the Static and Dynamic Stability Characteristics of a 10° Semivertex Angle Blunted Cone. NASA TN D-1202, 1962.

9. Intrieri, Peter F.: Free-Flight Measurements of the Static and Dynamic Stability and Drag of a 10° Blunted Cone at Mach Numbers 3.5 and 8.5. NASA TN D-1299, 1962.

10. Peterson, Victor L.: Motions of a Short 10° Blunted Cone Entering a Martian Atmosphere at Arbitrary Angles of Attack and Arbitrary Pitching Rates. NASA TN D-1326, 1962.

11. Chapman, Dean R.: An Approximate Analytical Method for Studying Entry into Planetary Atmospheres. NASA TR R-11, 1958. (Supersedes NACA TN 4276)

12. Yee, Layton, Bailey, Harry E., and Woodward, Henry T.: Ballistic Range Measurements of Stagnation-Point Heat Transfer in Air and in Carbon Dioxide at Velocities Up to 18,000 Feet Per Second. NASA TN D-777, 1961.

13. Hoshizaki, H.: Heat Transfer in Planetary Atmospheres at Super-Satellite Speeds. ARS Jour., vol. 32, no. 10, Oct. 1962, pp. 1544-52.

14. Lees, Lester: Laminar Heat Transfer Over Blunt-Nosed Bodies at Hypersonic Flight Speeds. ARS Jour., vol. 26, no. 4, April 1956, pp. 259-69.

15. Kivel, B., and Bailey, K.: Tables of Radiation from High Temperature Air. Res. Rep. 21, Avco Res. Lab., 1957.

16. Page, William A., Canning, Thomas N., Craig, Roger A., and Stephenson, Jack D.: Measurements of Thermal Radiation of Air From the Stagnation Region of Blunt Bodies Traveling at Velocities up to 31,000 Feet Per Second. NASA TM X-508, 1961.

17. Yoshikawa, Kenneth K., and Wick, Bradford H.: Radiative Heat Transfer During Atmosphere Entry at Parabolic Velocity. NASA TN D-1074, 1961.

18. Seiff, Alvin: Recent Information on Hypersonic Flow Fields. NASA SP-24, 1962, pp. 19-32.

19. Wick, Bradford H.: Radiative Heating of Vehicles Entering the Earth's Atmosphere. Presented to the Fluid Mechanics Panel of AGARD, Brussels, Belgium, April 1962.

20. Canning, Thomas N.: Recent Developments in the Chemistry and Thermodynamics of Gases at Hypervelocities. NASA SP-24, 1962, pp. 33-40.

21. Romig, Mary F.: Conical Flow Parameters for Air in Dissociation Equilibrium: Final Results. Convair Research Note 14, 1958.

22. Stephenson, Jack D.: A Technique for Determining Relaxation Times By Free-Flight Test of Low-Fineness-Ratio Cones, With Experimental Results for Air At Equilibrium Temperatures Up to 3440° K. NASA TN D-327, 1960.

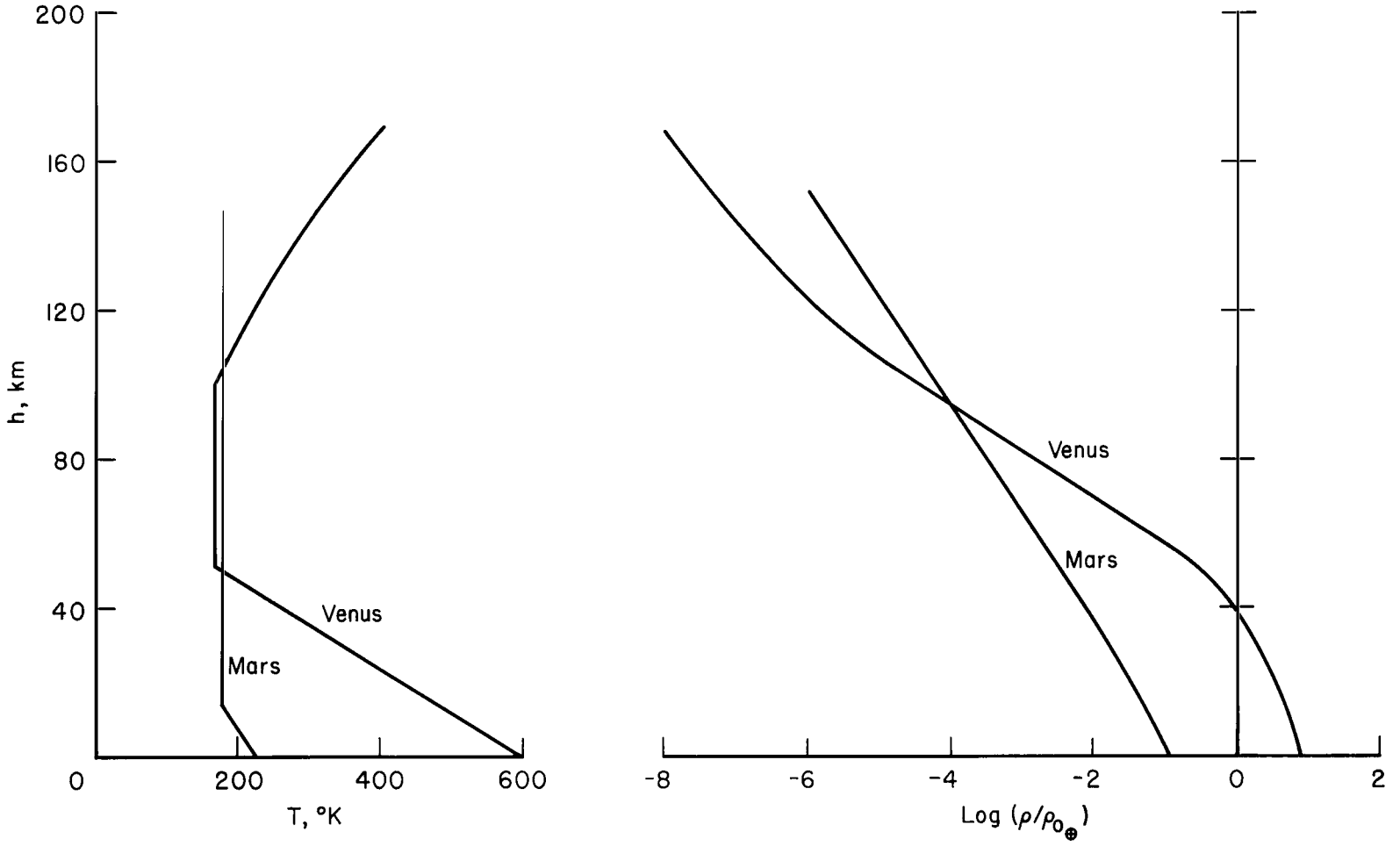

(a) Temperature.

(b) Density ratio.

Figure 1.- Temperature and density profiles of assumed model atmospheres.

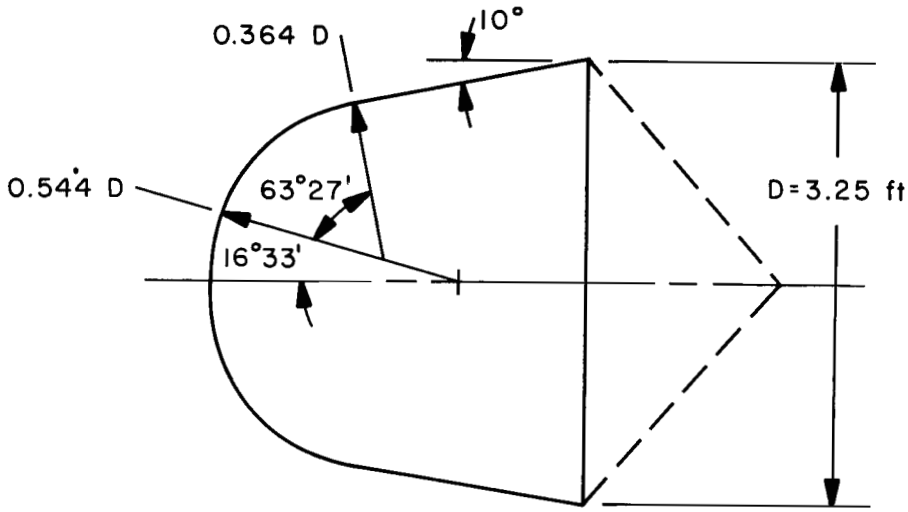

(a) Blunt capsule.

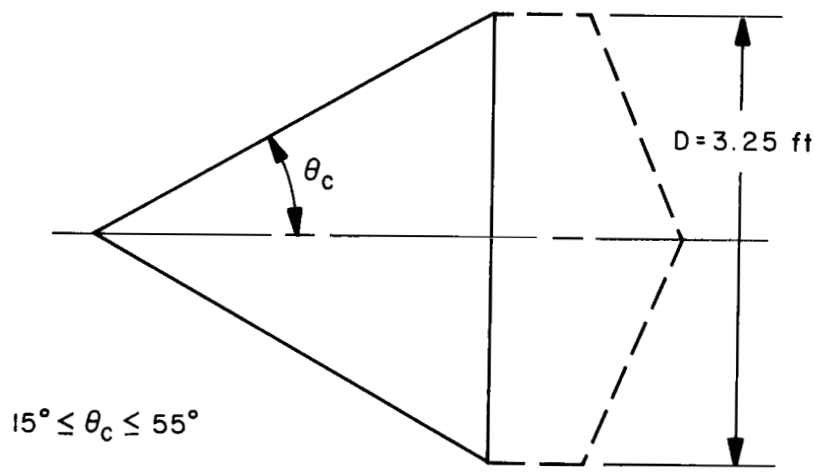

(b) Conical shapes.

Figure 2.- Shapes considered.

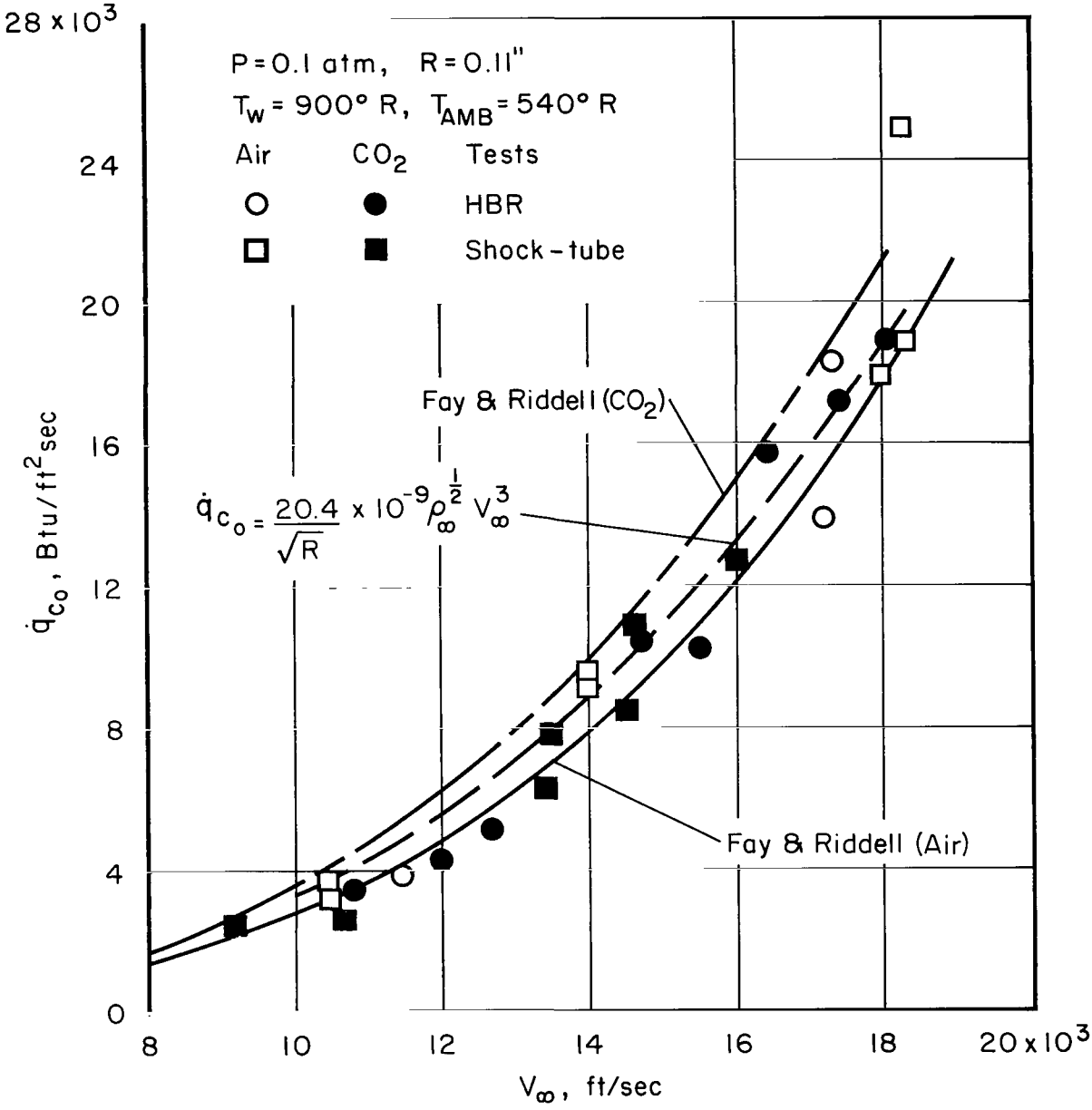

Figure 3.- Comparison of theoretical and experimental stagnation convective heating rates.

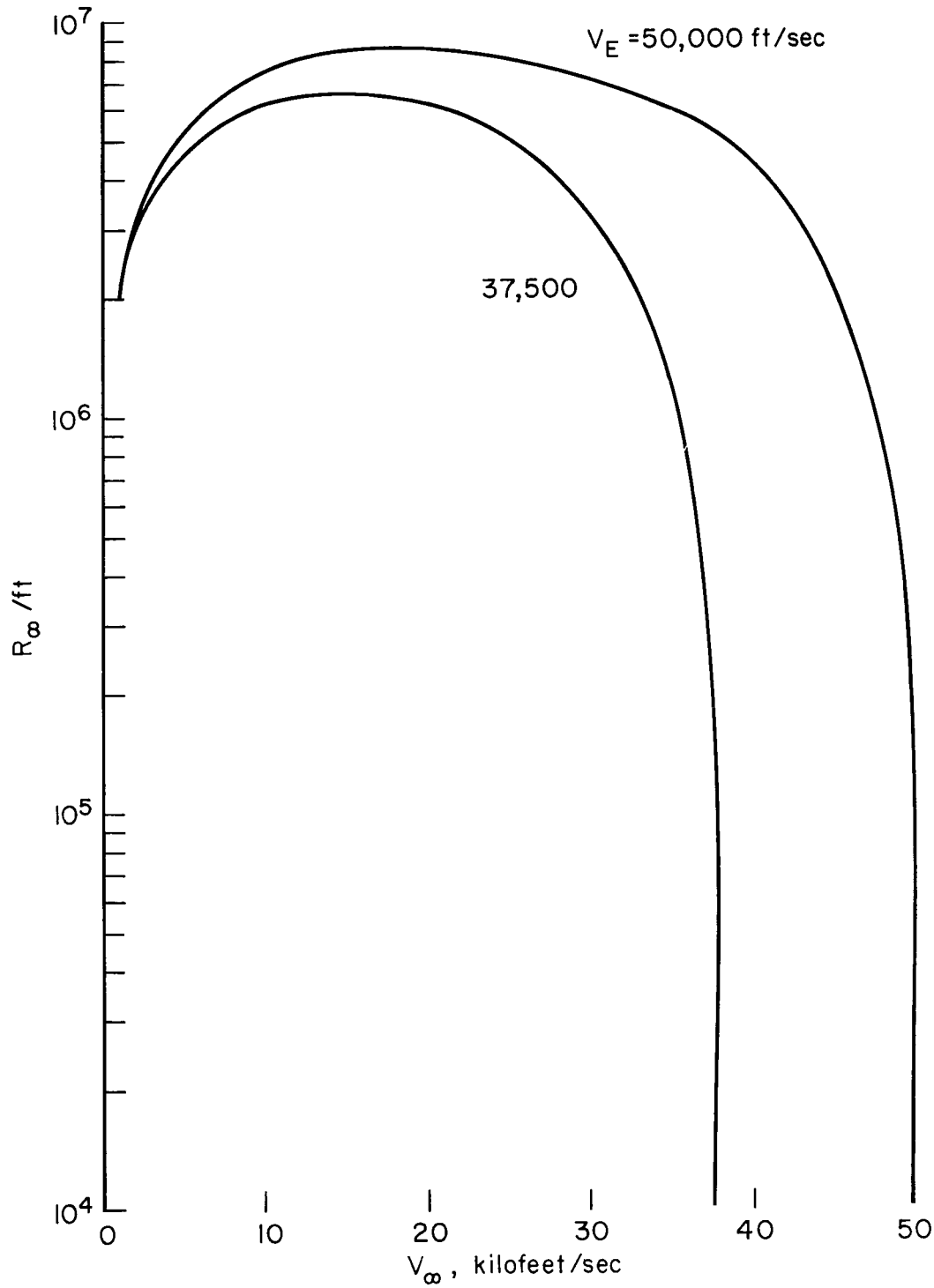

(a) Venus entries.

Figure 4.- Reynolds numbers encountered during entry $\gamma_E = -89^\circ$, $\frac{m}{C_D A} = 1$ slug/ft^2.

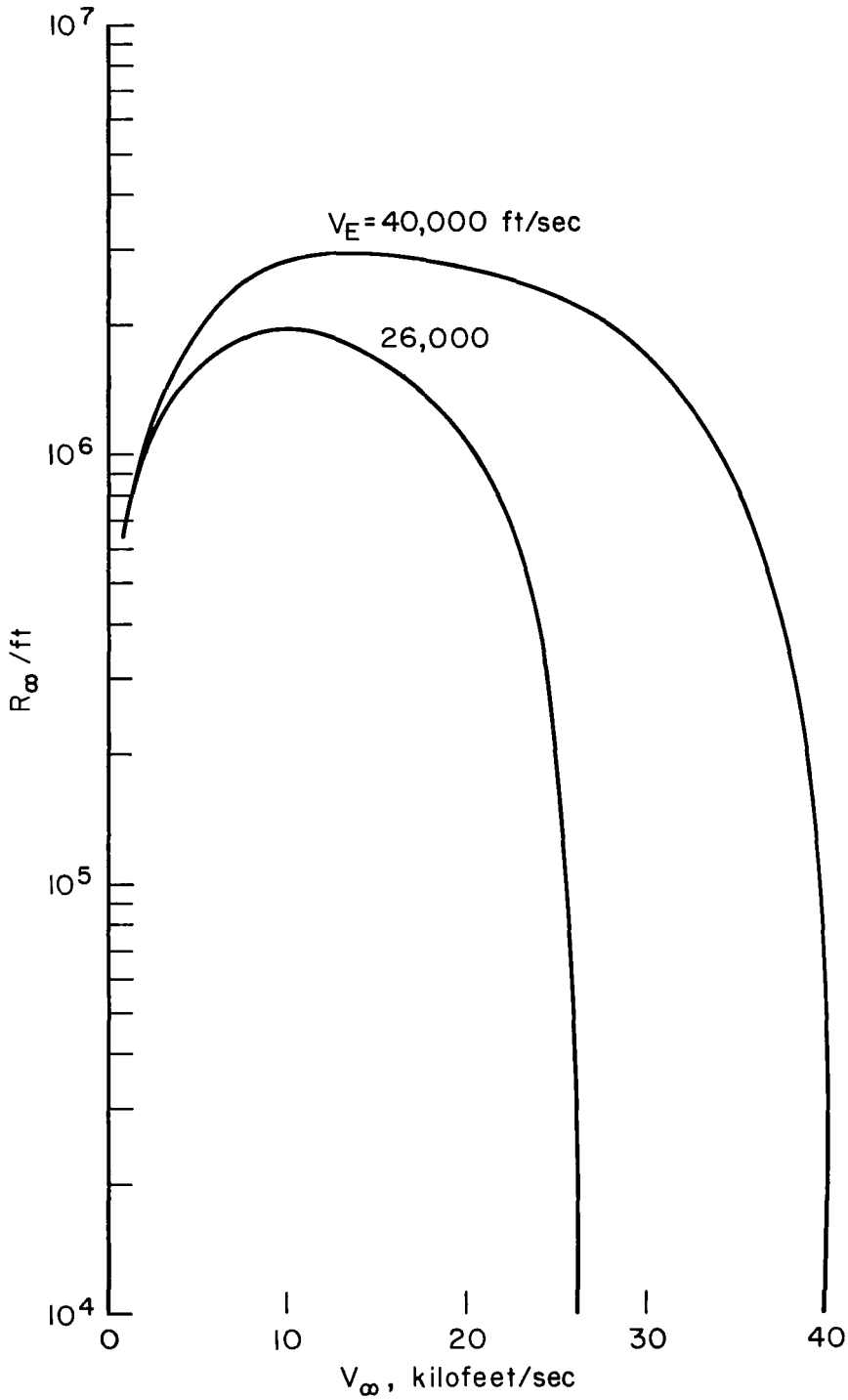

(b) Mars entries.

Figure 4.- Concluded.

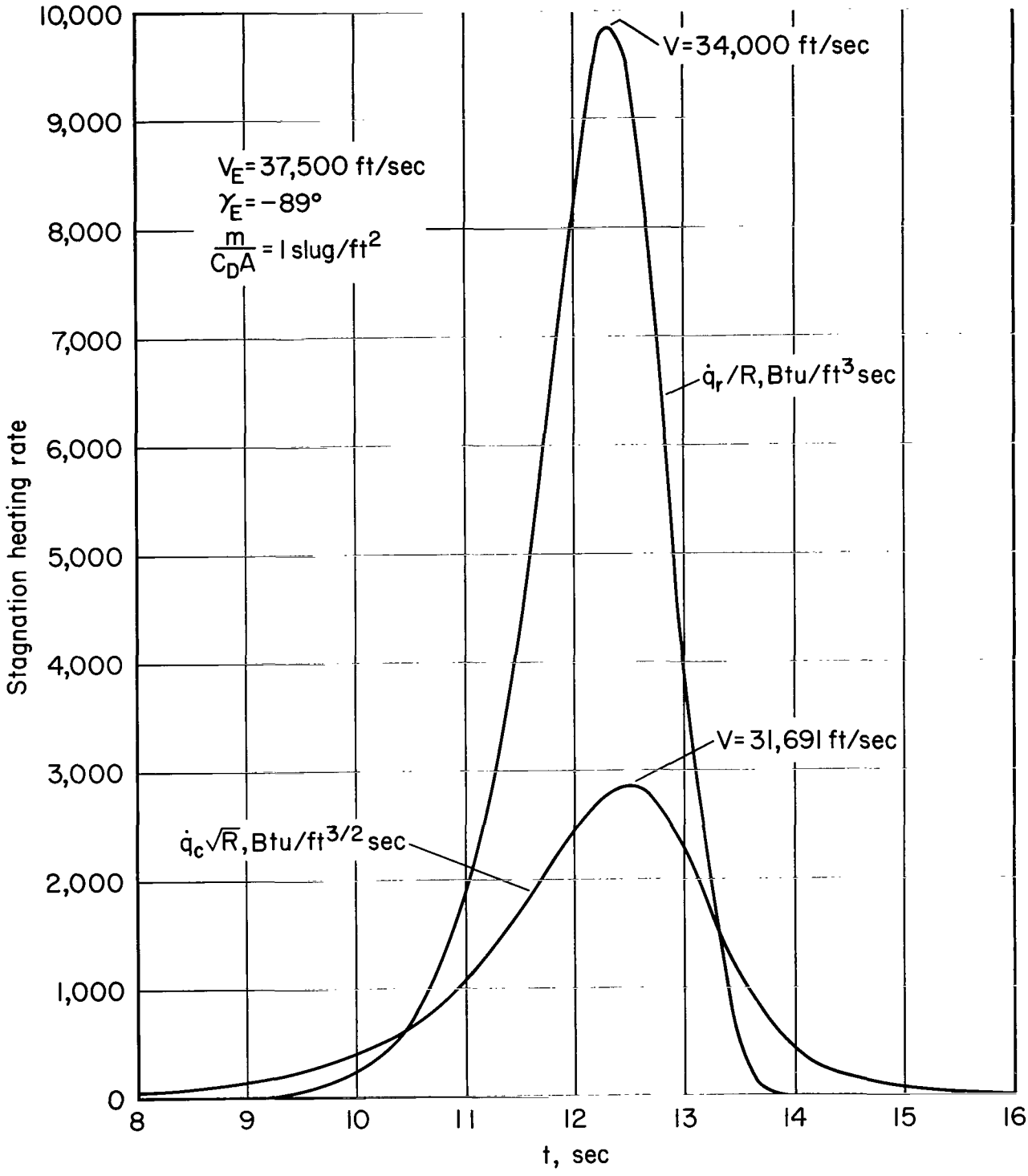

(a) Venus entry.

Figure 5.- Stagnation-point heating rates for blunt capsule.

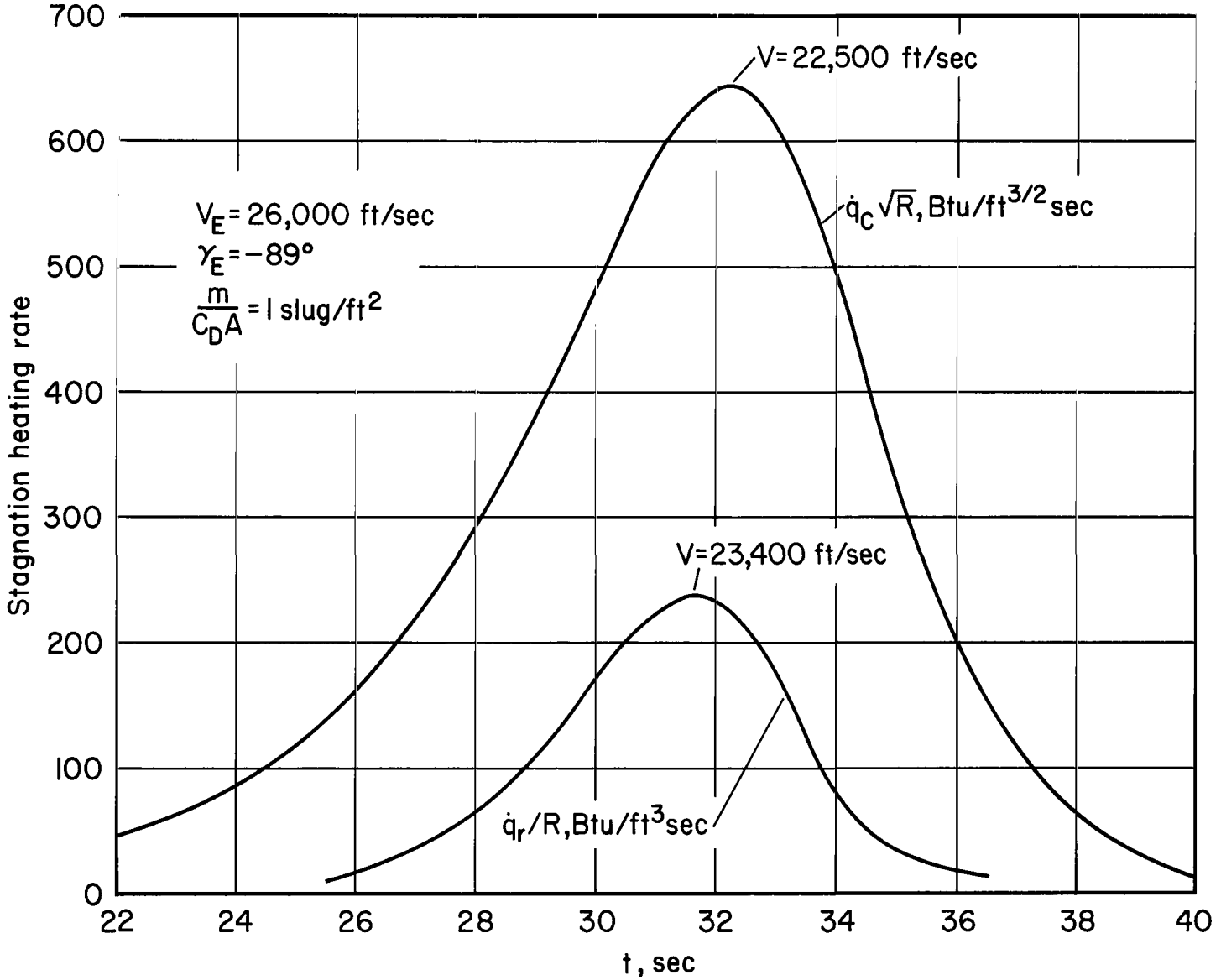

(b) Mars entry.

Figure 5.- Concluded.

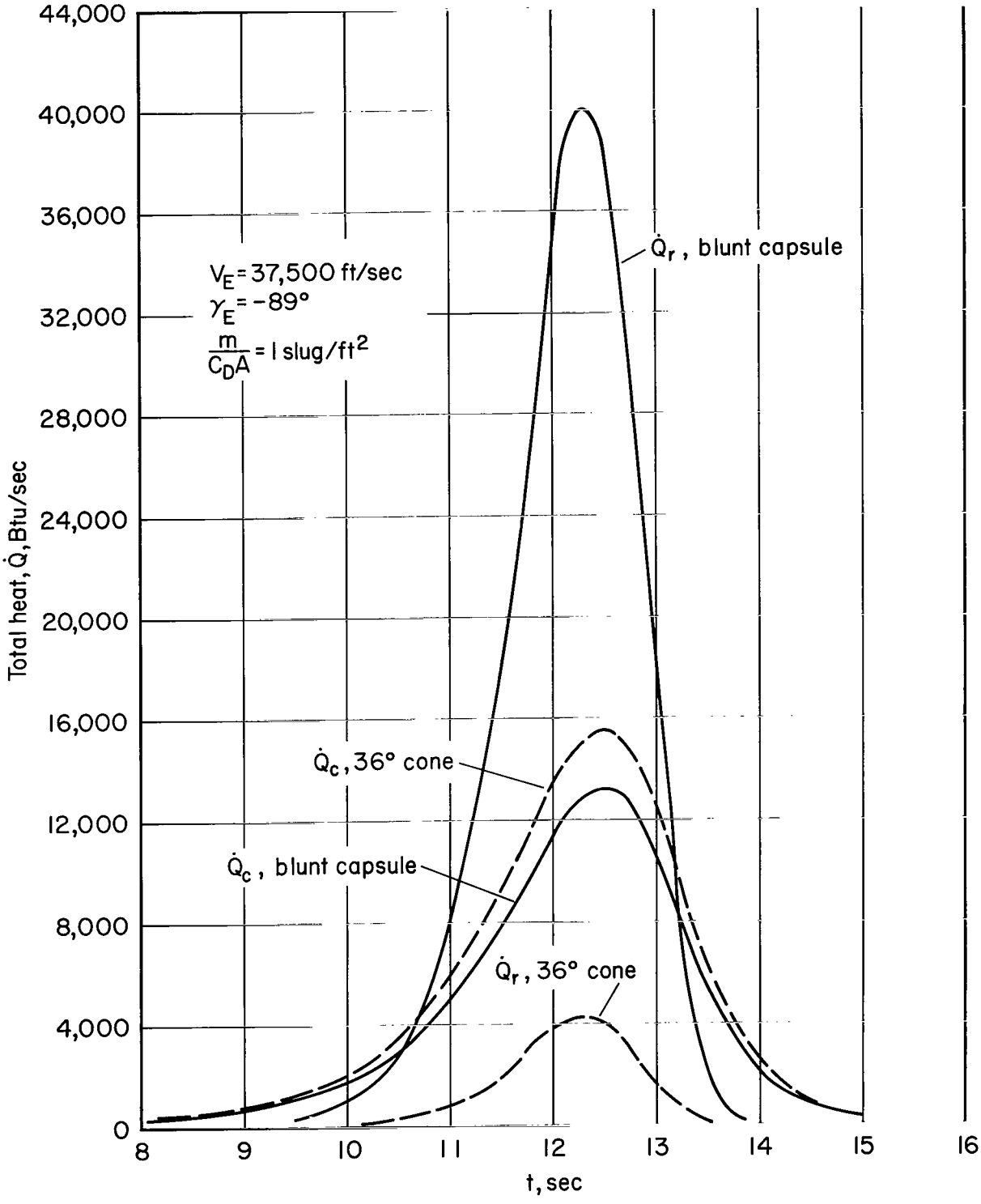

(a) Venus entry.

Figure 6.- Time histories of convective and radiative heat inputs; D = 3.25 ft.

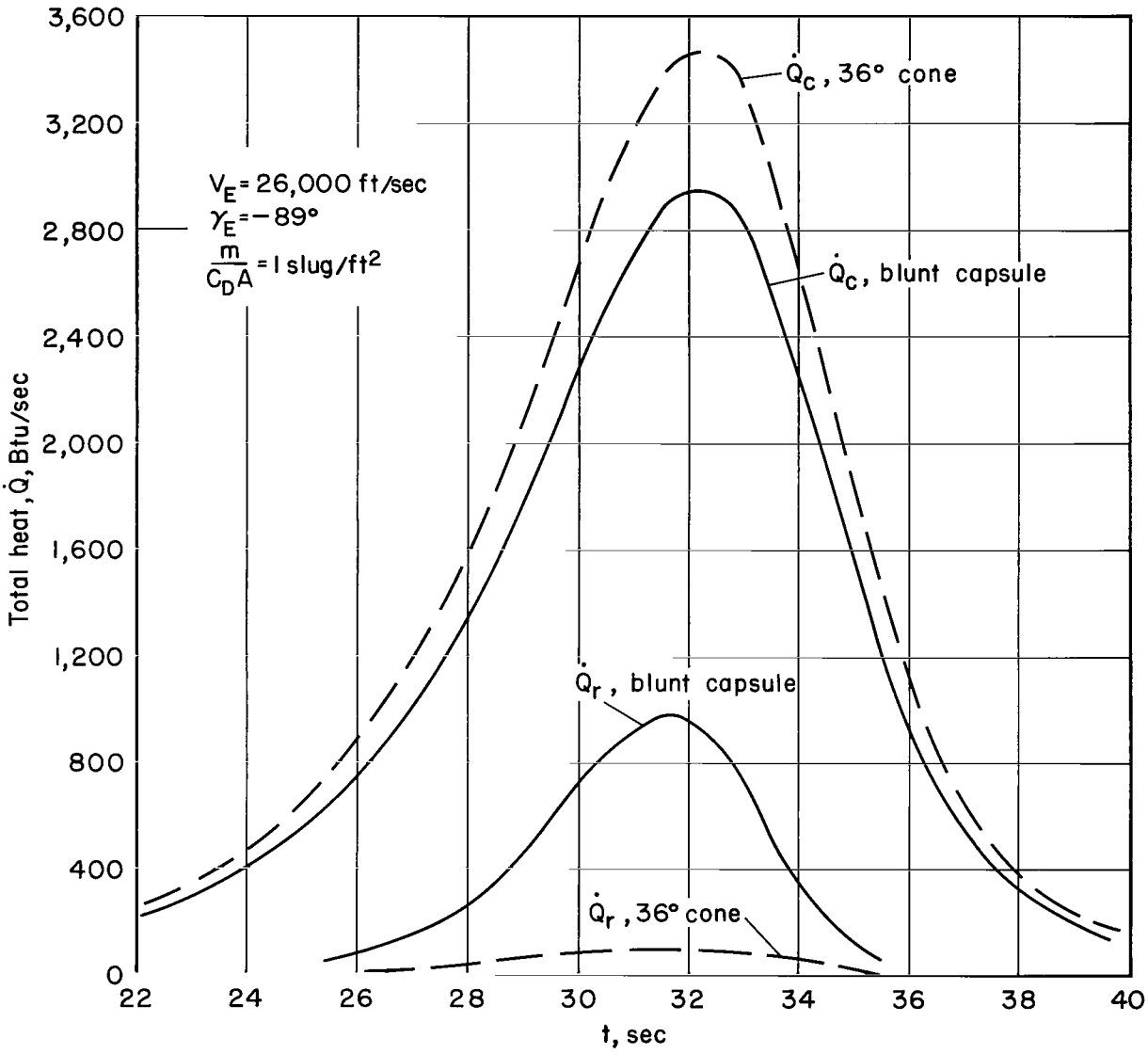

(b) Mars entry.

Figure 6.- Concluded.

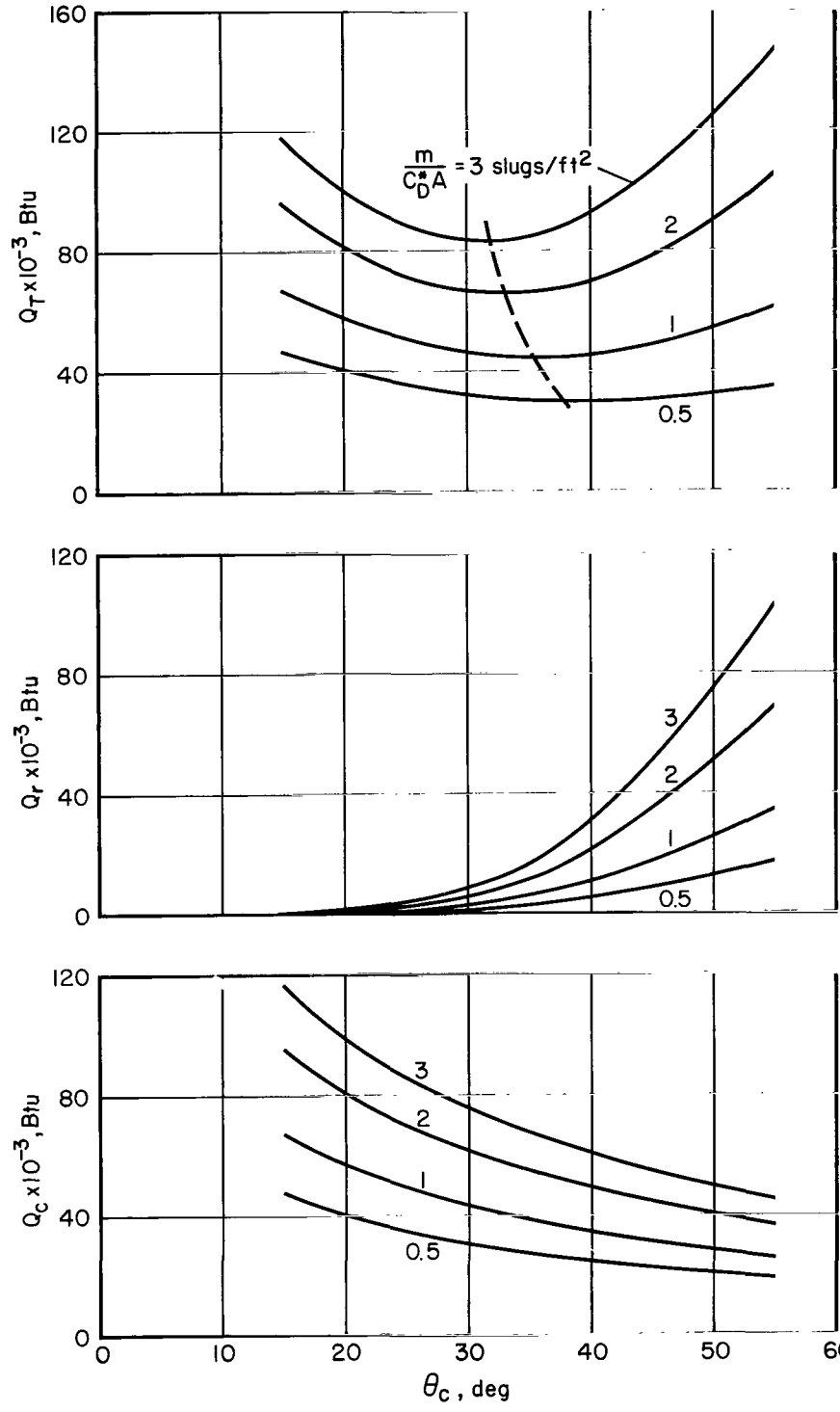

(a) V_E = 37,500 ft/sec.

Figure 7.- The variation of heat inputs with cone angle for Venus entry; D = 3.25 ft.

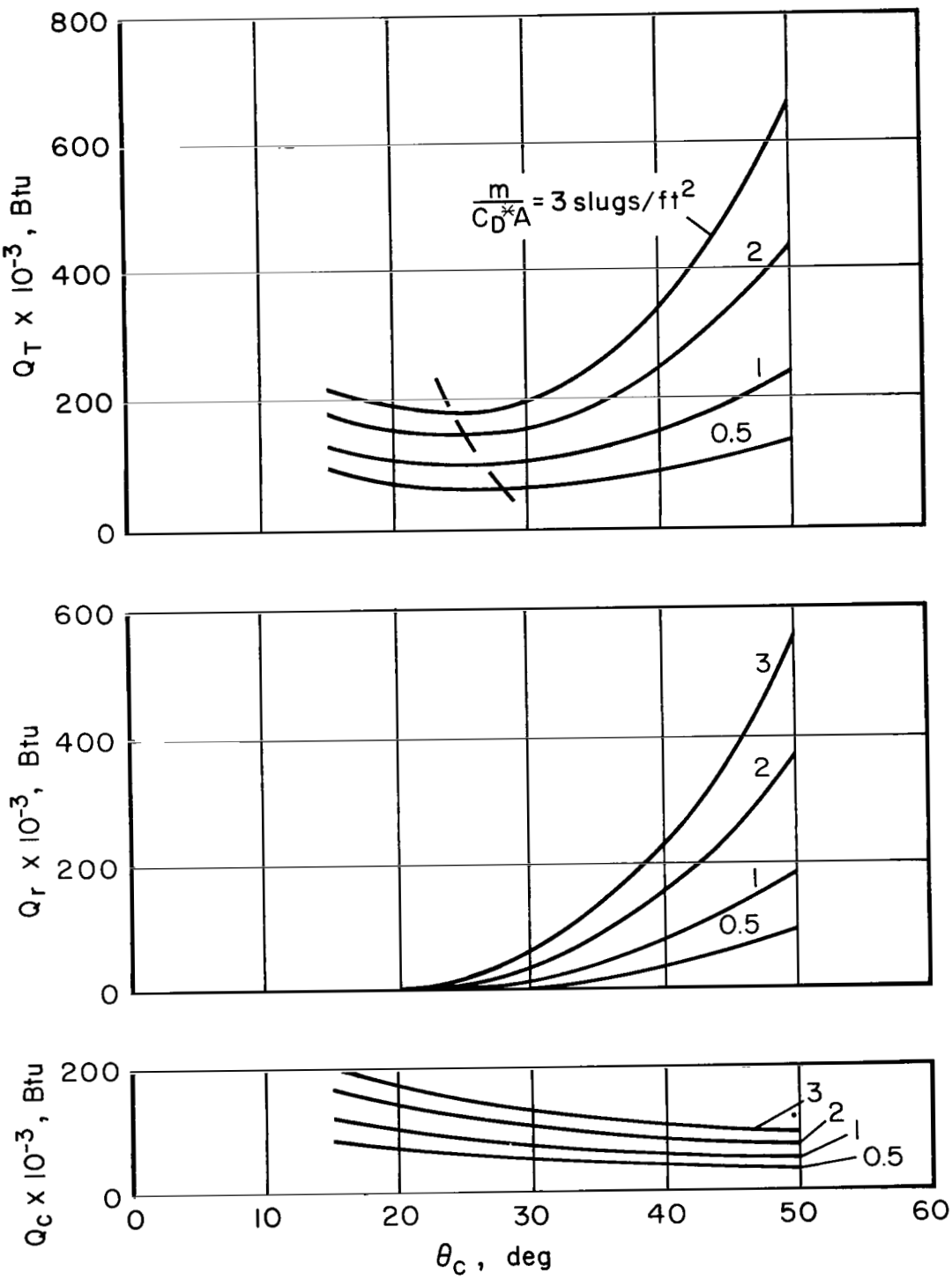

(b) V_E = 50,000 ft/sec.

Figure 7.- Concluded.

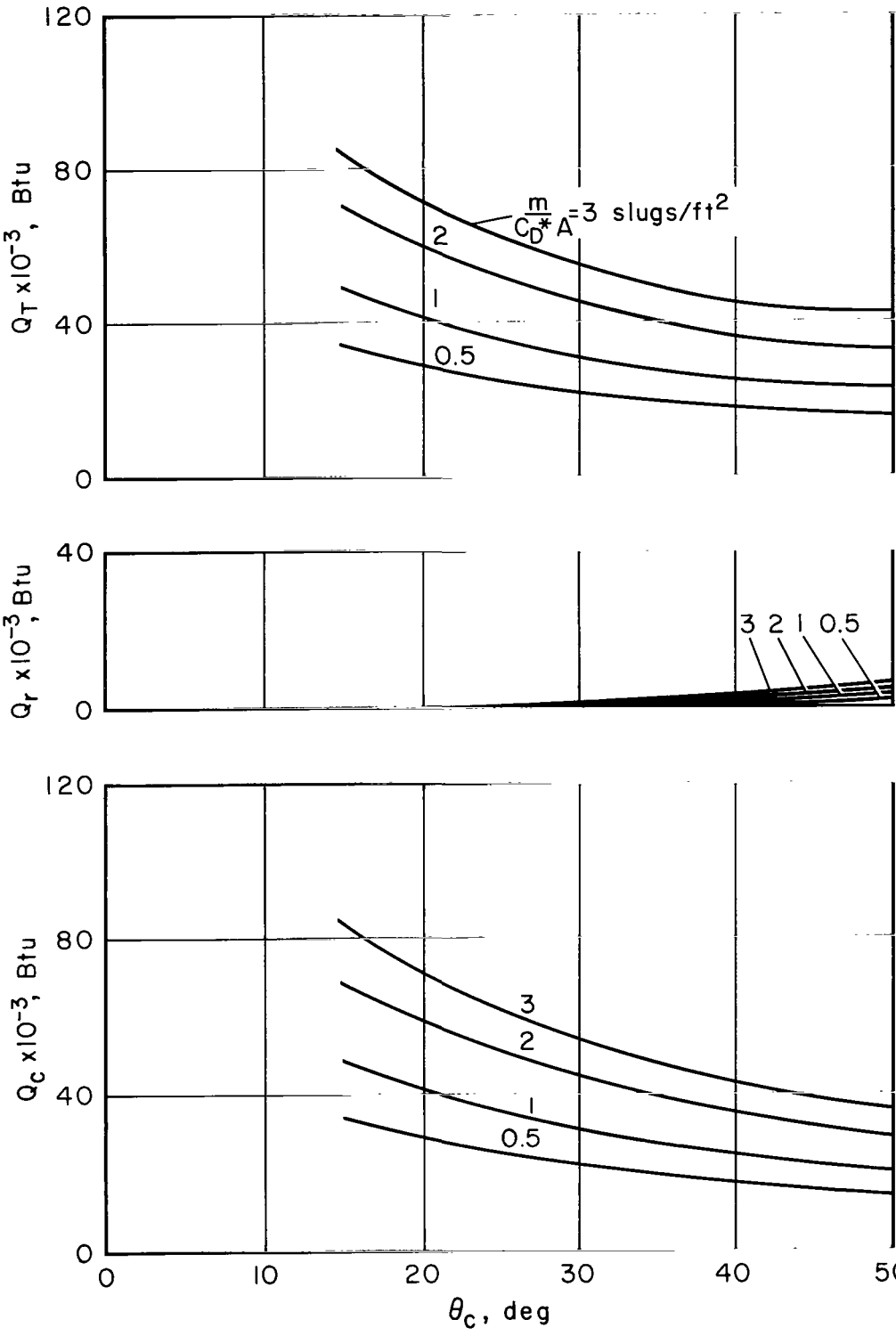

(a) V_E = 26,000 ft/sec.

Figure 8.- The variation of heat inputs with cone angle for Mars entry; D = 3.25 ft.

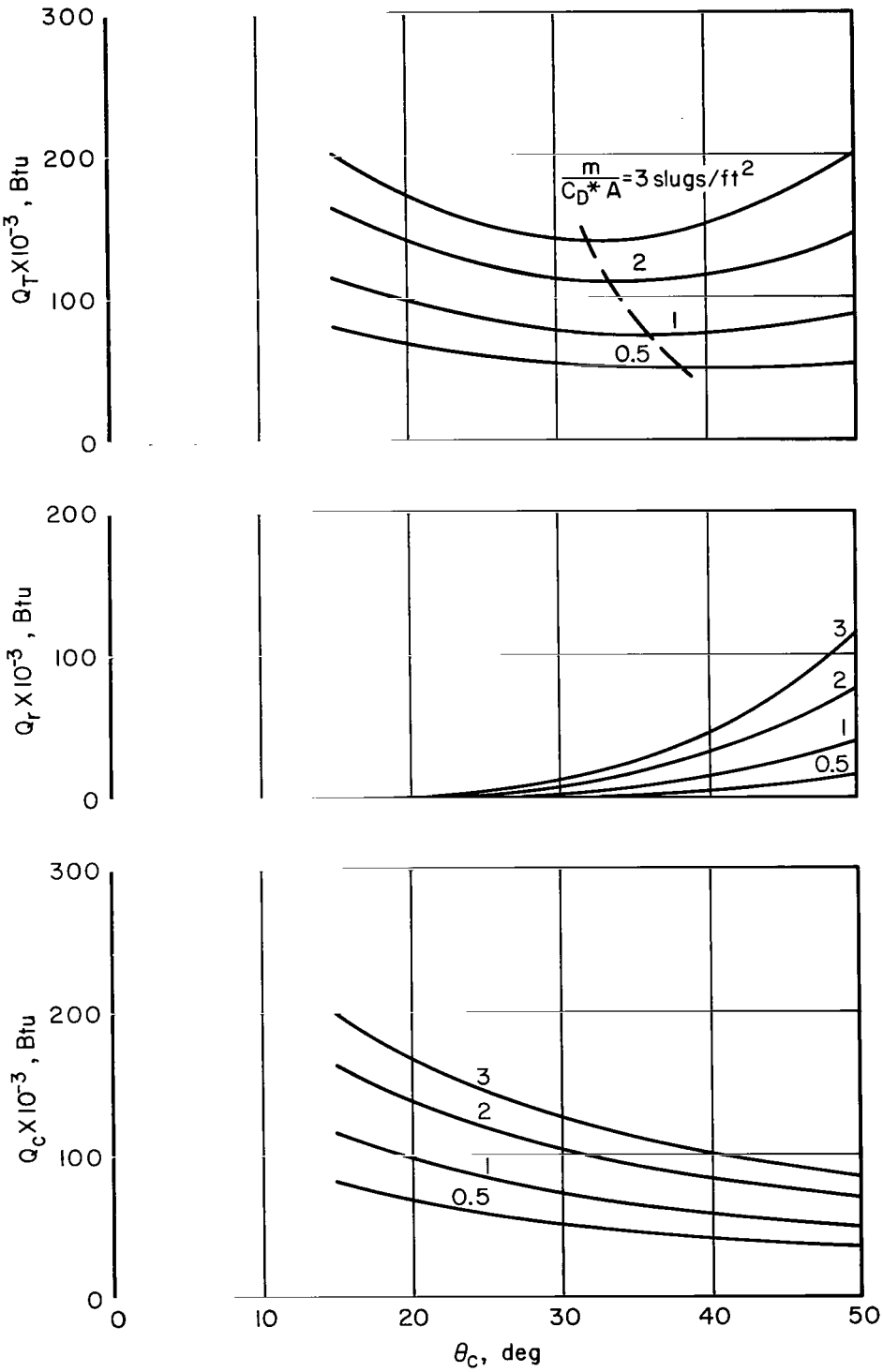

(b) V_∞ = 40,000 ft/sec.

Figure 8.- Concluded.

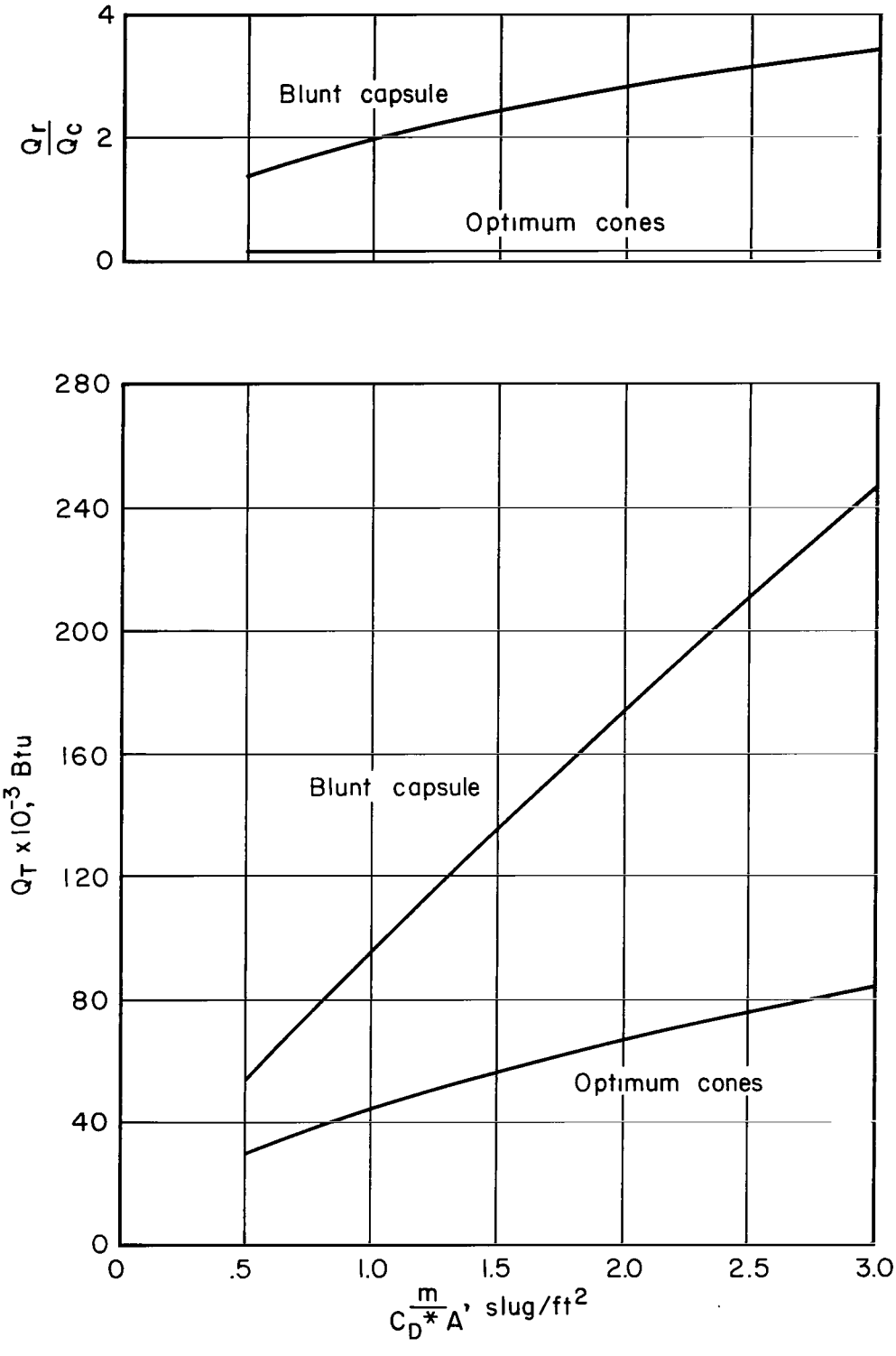

(a) Venus, V_E = 37,500 ft/sec.

Figure 9.- Comparison of heat inputs to blunt capsule and to optimum cones; D = 3.25 ft.

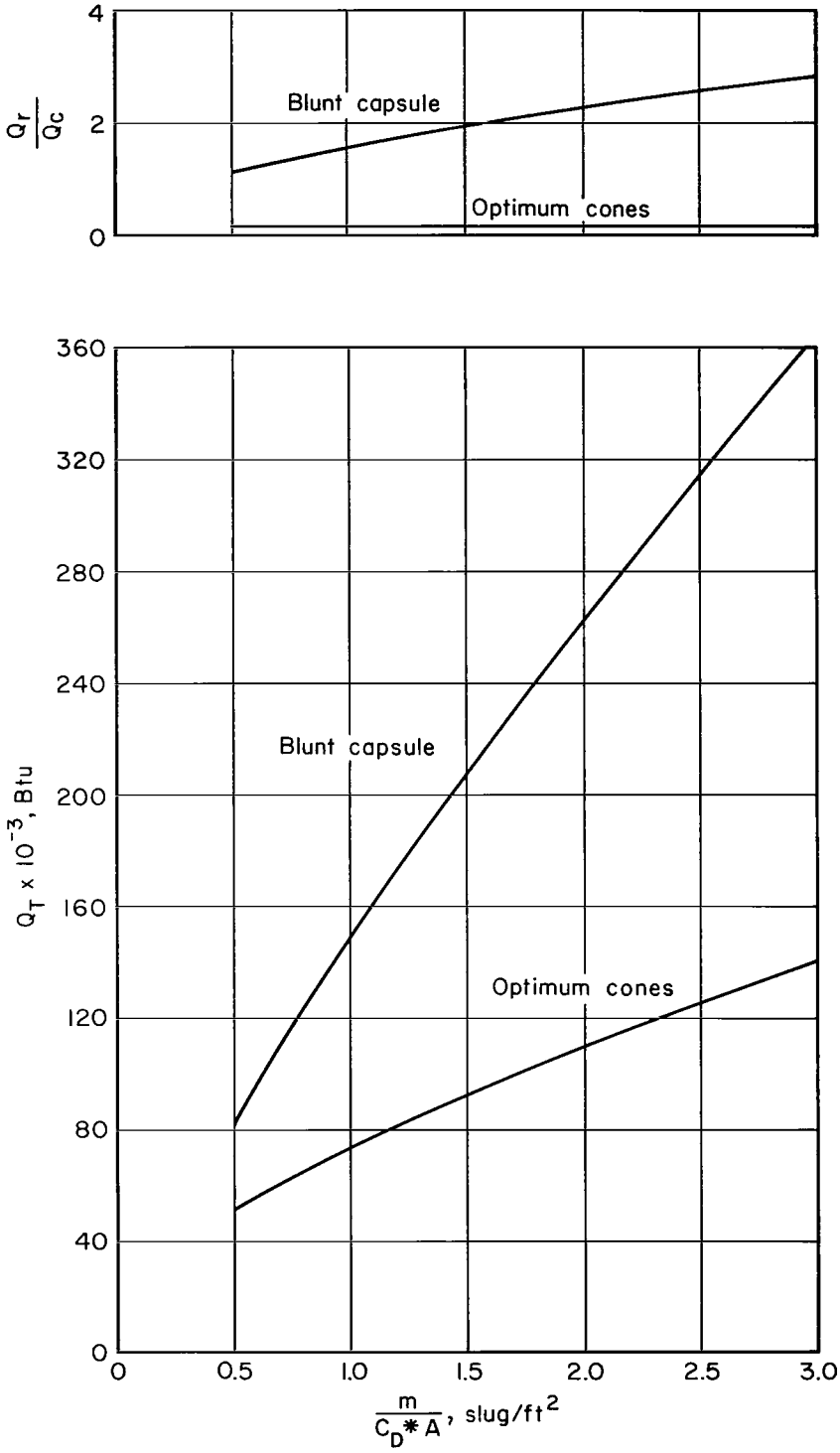

(b) Mars, V_E = 40,000 ft/sec.

Figure 9.- Concluded.

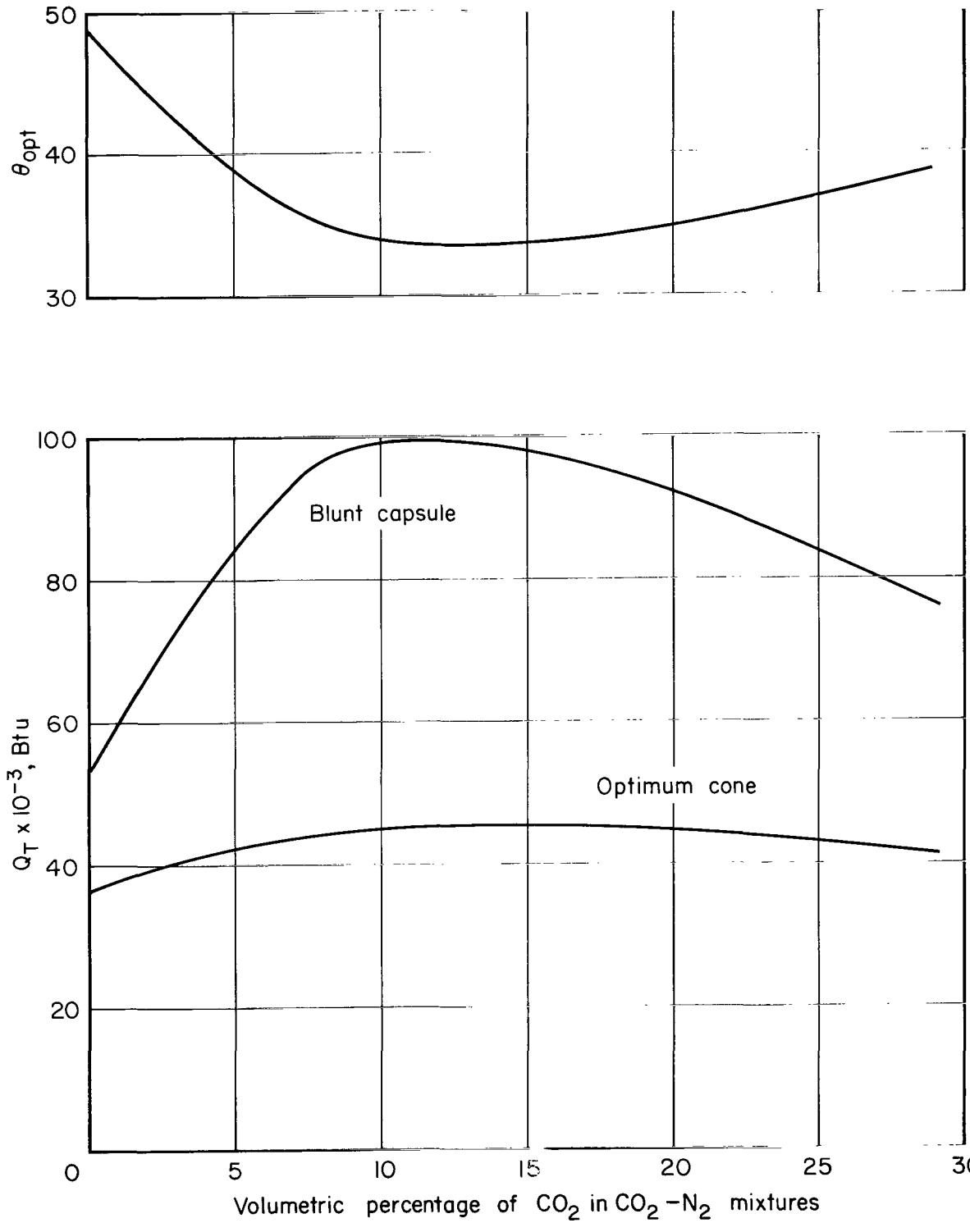

Figure 10.- Effect of gas composition on total heat characteristics for Venus entry at 37,500 ft/sec; m/C_D*A = 1 slug/ft^2; D = 3.25 ft.

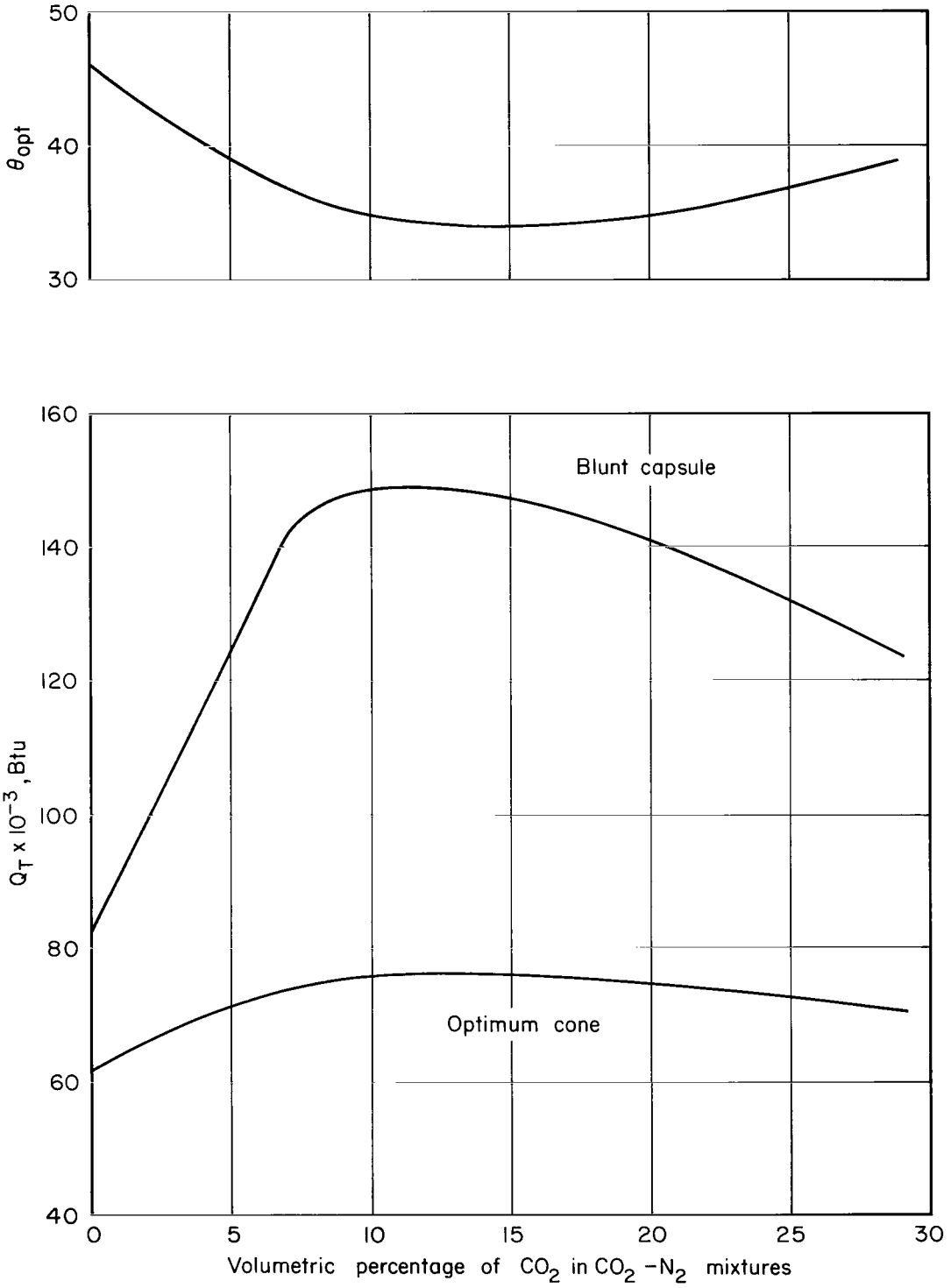

Figure 11.- Effect of gas composition on total heat characteristics for Mars entry at 40,000 ft/sec; m/C_D*A = 1 slug/ft^2; D = 3.25 ft.